International Journal of Minerals, Metallurgy and Materials
Volume 28, Number 12, December 2021, Page 1991
https://doi.org/10.1007/s12613-020-2122-0

Hydrothermal synthesis of Zn–Mg-based layered double hydroxide coatings for the corrosion protection of copper in chloride and hydroxide media

Nikhil [1)], *Gopal Ji*[1,2)], *and Rajiv Prakash*[1)]

1) School of Materials Science and Technology, Indian Institute of Technology (BHU) Varanasi, Varanasi-221005, Uttar Pradesh, India
2) Centre for advanced studies, Dr. APJAKTU Lucknow, U.P. -226031, India
(Received: 3 March 2020; revised: 4 June 2020; accepted: 18 June 2020)

Abstract: Layered double hydroxides (LDHs) hinder corrosive elements by forming a double layer and locking them between its layers. Hence, LDHs are interesting materials in corrosion inhibition. In this work, Zn–Mg-based LDHs are grown over a copper substrate by using a hydrothermal method. Two types of Zn–Mg-based LDH coating are prepared based on hydrothermal reaction time. Both types are characterized through Fourier transform infrared spectroscopy, Raman spectroscopy, high-resolution scanning electron microscopy, energy dispersive X-ray analysis, atomic force microscopy, and X-ray diffraction. Results show that the two types of LDH coating are successfully grown on copper; however, they differ in thickness and structural configuration. Corrosion testing of the LDH coatings is executed in 0.1 M NaCl and 0.1 M NaOH through alternating current impedance measurements and Tafel polarization curves. Results show that L48 gives more than 90% protection to copper, which is higher than the protection provided by L24. However, both LDH coatings (L24 and L48) are more effective corrosion inhibitors in NaCl than in NaOH, suggesting that the LDH coatings can more efficiently exchange Cl ions than OH ions.

Keywords: hydrothermal synthesis; layered double hydroxides; anticorrosion coating; ion exchange; copper substrate

1. Introduction

Copper-based equipment exhibits great physical, mechanical, thermal, electrical, antimicrobial, and corrosion-resistant properties [1–2]. Copper loss due to corrosion is usually low in most working media; however, aggressive molecules can cause copper loss at a faster rate than usual [3–4]. Hence, prevention of copper from attacking molecules is necessary. Copper can be protected against deterioration through many methods, the most effective of which are the use of inhibitive materials in working media and coatings of inhibitive materials over metal substrates [5–8]. Inhibitors and coatings differ in that inhibitors form a protective layer on the metal substrate after being adsorbed on it, whereas coatings provide a preformed inhibitive layer on the metal substrate. In both cases, the inhibitive layer provides protection to underneath metal substrate. However, inhibitive coatings are preferred over inhibitors, and stable protection of copper-based equipment is given focus.

Various types of inhibitive materials have been used for coating applications. Layered double hydroxides (LDHs) are generally used for copper protection because of their specific structure. LDHs have a unified formula of $[M^{2+}_{1-x}, M^{3+}_{x}(OH)_2]^{x+} A^{n-}_{x/2} mH_2O$, where M^{2+} and M^{3+} are metal cations and A^{n-} is an anion located between metallic layers. Given their unique structure, LDHs can exchange the anion of the environment with its anion (intercalated between layers of metal cations) and thus can reduce the aggressiveness of the environment. LDHs can also store and release inhibitors for extra protection against corrosion. As such, LDHs have also been used to produce nanocontainers and nanocomposite anticorrosion coatings [9–11]. In addition, LDHs feature high bio-compatibility, low toxicity, chemical inertness, and good antibacterial properties [12]. Given these unique properties, LDHs have been used for the corrosion protection of metals [12–14]. However, LDHs for metal protection have been based on either Zn–Al or Al–Mg [13–16]. A general requirement of LDHs is that one cation should be divalent and another cation should be trivalent. In normal LDHs, aluminum is used as a trivalent cation while Zn/Mg is used as a divalent cation. However, LDHs with divalent cations at both places have never been synthesized and used for copper protection. In the present work, Zn^{2+} and Mg^{2+} are used as metal cations for the *in situ* synthesis of LDH coatings to evaluate the pro-

Corresponding author: Gopal Ji E-mail: gopal.ji.ji@gmail.com; gopalji@cas.res.in

tection ability of LDH coatings with only divalent cations. In addition, two types of Zn–Mg-based LDH coating are synthesized by using two reaction times of 24 h (L24) and 48 h (L48). The effects of changes in the LDH coatings on the inhibition potential are then determined.

This study aimed to synthesize Zn–Mg-based LDH coatings over a copper substrate for corrosion prevention in 0.1 M NaCl and 0.1 M NaOH at room temperature (24±2°C). The chloride and hydroxide media are used to test the stability of LDH coatings in opposite conditions. Both LDH coatings (L24 and L48) are characterized through Fourier transform infrared (FTIR) spectroscopy, Raman spectroscopy, high-resolution scanning electron microscopy (HRSEM), energy dispersive X-ray analysis (EDAX), atomic force microscopy (AFM), and X-ray diffraction (XRD). Corrosion tests on the LDH-coated copper substrates are performed using alternating current (AC) impedance measurements (AIM) and Tafel polarization curves (TPC). Results show that LDHs are an effective barrier against corrosion on copper in both media.

2. Experimental

2.1. Synthesis of Zn–Mg based LDHs

Zn–Mg-based LDHs were prepared in accordance with the procedure described by Zeng *et al.* [13]. Initially, $Zn(NO_3)_2{\cdot}6H_2O$ and $Mg(NO_3)_2{\cdot}6H_2O$ were mixed in a molar ratio of 2:1 in 50 mL of deionized (DI) water and referred as "solution A." Solution B was prepared by mixing Na_2CO_3 and NaOH in a molar ratio of 1:3 in 50 mL of DI water. Solution A was continuously stirred, and solution B was gradually added into it. The resultant mixture was stirred at 65°C for 48 h. The obtained mixture was cooled down to room temperature. Then, the cooled mixture was poured into a Teflon-lined autoclave to submerge a copper strip of 5 cm × 5 cm. This procedure was performed for the *in situ* growth of LDHs over the copper substrate. Furthermore, the autoclave was heated at 120°C for 24 and 48 h. Thus, two Zn–Mg-based LDHs (L24 and L28) were synthesized over the copper substrate by varying the reaction time.

2.2. Characterization of LDHs

Prior to the growth of LDHs, the copper strip (5 cm × 5 cm) was cleaned with ethanol-soaked tissue paper. The clean copper strip was then ground sequentially with 1/0–5/0-grade emery paper (Sianor b, Switzerland) for 5 min. Again, the strips were cleaned by ethanol and compressed air. Thus, the prepared strips were placed in the autoclave for the growth of LDHs over it. After the growth of L24 and L48 over copper, the coated copper strips were washed thrice with DI water. Then, three strips of size 3 cm × 1 cm were cut from the coated strips and used in corrosion testing. All other tests were performed on LDH-coated strips of 1 cm × 1 cm size. High-resolution surface micro-images of the LDH-coated strips were recorded by Nova Nano Sem 450 FEI (U.S.A.) equipped with an EDAX analyzer. The XRD patterns of the LDH-coated copper substrate were obtained using a Miniflex 600 diffractometer with copper K_α X-rays (wavelength =15.406 nm). FTIR analysis of the coated strips was performed in attenuated total reflectance (ATR) mode on a Thermo Nicolet Nexus 5700. Raman spectrum was recorded using an SPR 300 Raman spectrometer (laser source, 532 nm). AFM topographies were recorded under tapping mode by using an NT-MDT (NTEGRA Prima) instrument.

2.3. Corrosion analysis

For corrosion testing, only 1 cm^2 of the 3 cm × 1 cm coated strips was exposed to the test solution by masking the rest of the surface with 3 M polyester tape. Thus, the prepared strips (working electrodes) were hung in test solutions (0.1 M NaCl and 0.1 M NaOH) along with silver/silver chloride (reference) and platinum (auxiliary) tubular electrodes. The corrosion test was performed after immersing the specimens in the test solution for 1 h to consider the initial fluctuation of the working electrode after immersion in the test solution.

For AIM, an AC signal of 5 mV root mean square (RMS) amplitude was generated between 10^5 and 10^{-2} Hz (10 frequency per decade) with the help of NOVA 1.11 and applied to the system under investigation by Metrohm PGSTAT 302. For TPC, the system was scanned within open circuit potential (OCP) ±250 mV (vs. reference electrode) at the rate of 5 mV/s. The impedance spectra and TPC were fitted by Zsim and CHI-7041 C, respectively. The inhibition efficiency was calculated using the values obtained by fitting as given below [17–19]:

$$\eta_{\mathrm{Rct}}(\%) = \frac{R_{\mathrm{ct}}^{\mathrm{i}} - R_{\mathrm{ct}}^{0}}{R_{ct}^{\mathrm{i}}} \times 100 \quad (1)$$

$$\eta_{\mathrm{Pl}}(\%) = \frac{i_{\mathrm{corr}}^{0} - i_{\mathrm{corr}}^{\mathrm{i}}}{i_{\mathrm{corr}}^{0}} \times 100 \quad (2)$$

where η_{Rct} is the charge transfer-based inhibition efficiency and η_{Pl} is the polarization-based inhibition efficiency. R_{ct}^{0} and i_{corr}^{0} are the charge transfer resistance and corrosion current density in the test solutions, respectively, and $R_{\mathrm{ct}}^{\mathrm{i}}$and $i_{\mathrm{corr}}^{\mathrm{i}}$ are those of the LDH-coated copper strips in the test solutions.

3. Results and discussion

LDH coatings were grown (*in situ*) on a copper substrate through a hydrothermal method. Real images of the L24- and L48-coated copper substrates are shown in Fig. 1. The thicknesses of copper and the LDH-coated copper were measured at eight places on one sample by using a Mitutoyo absolute AOS digimatic caliper (made in U.S.A., least count- 10 μm),

which are given as follows: copper, 44±3 μm; L24, 51±4 μm; L48, 59±2 μm. This result indicated that the coating thickness increased with reaction time. These coatings were characterized using various techniques to confirm the formation of LDH coatings over the copper substrate.

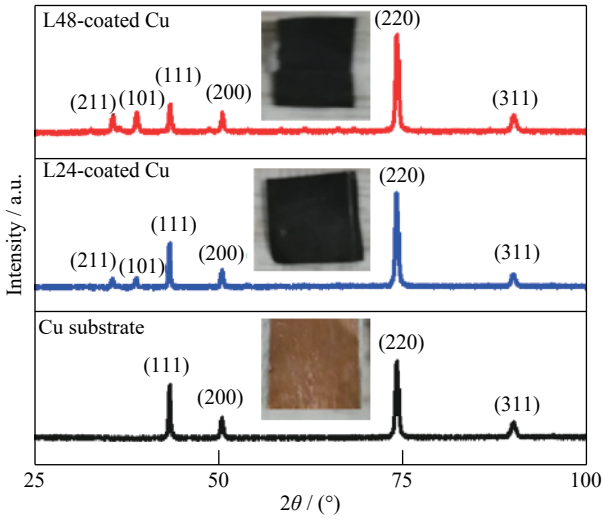

Fig. 1. XRD patterns of polished copper, L24, and L48 LDH coatings.

3.1. Characterization of LDH-coated copper substrate

3.1.1. XRD analysis

Fig. 1 shows the XRD patterns of the copper and LDH-coated (L24 and L48) copper substrates. The copper showed various peaks in its XRD pattern, which corresponded to important peaks of copper (JCPDS file No. 85-1326) and confirmed that the substrate used in the process was standard copper. Due to hydrothermal treatment, two new peaks appeared at 35.6° and 38.8° in the LDH-coated copper substrates. In addition, the (111) peak intensity of copper (43.2°) decreased with reaction time of LDH, i.e., higher for L24 and lower for L48. These findings indicated the formation of Zn–Mg-based LDHs on the copper substrates. Close observation of the XRD patterns showed that the peak intensities at 35.6° and 38.8° were higher in the L48-coated copper than in the L24-coated copper. This result suggests that L24 and L48 have structural differences. Furthermore, the peaks at 38.8° (101) and 35.5° (211) corresponded to crystalline $Mg(OH)_2$ (JCPDS file No. 44-1482) and $Zn(OH)_2$ (JCPDS file No. 20-1437), respectively. The peak of the metal oxide can also be observed in the zoom view of the XRD patterns of LDHs (Fig. 2); however, it is not clearly noticed among other peaks in Fig. 1 because of its low intensity. This information clearly confirmed that Zn–Mg-based LDHs were grown on the copper substrates [20].

3.1.2. Spectroscopic analysis

Fig. 3 displays the FTIR spectra of the LDH-coated copper substrates captured in ATR mode. The absorption band

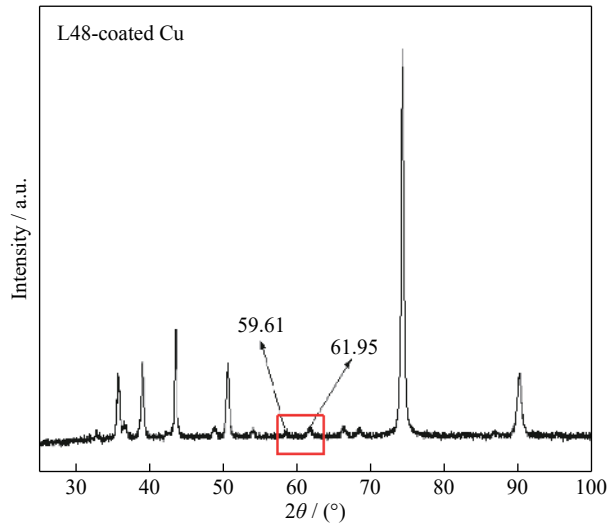

Fig. 2. Zoom view of XRD pattern of L48-coated copper.

around 3700 cm^{-1} corresponded to M–OH (Zn–OH/Mg–OH) stretching vibrations. The peak at 3600 cm^{-1} could be attributed to the O–H stretching of intercalated and adsorbed water molecules on the LDH surface. The band at 1700 cm^{-1} could correspond to the O–H bending vibration of water molecules. The bands at 1500, 1340, 1220, and 980 cm^{-1} were related to the symmetric and asymmetric stretching of CO_3^{2-} ion intercalated in the layers of the Zn–Mg-based LDHs. The band at 3000 cm^{-1} could be referred as CO_3^{2-}–H_2O bridging vibrations. The bands around 517 and 532 cm^{-1} in L24 corresponded to Zn–O and Mg–O stretching, whereas L48 showed these vibrations at 515 and 562 cm^{-1} [21].

Fig. 4 displays the Raman spectra of the LDH-coated copper substrates. The peaks of L48 were related to different stretching vibrations: 467 cm^{-1}, Zn–OH stretching; 550 cm^{-1}, Mg–OH stretching; 617 cm^{-1}, H_2O–CO_3^{2-}stretching; and 1126 cm^{-1}, CO_3^{2-} stretching. These stretching vibrations appeared in the L24-coated copper at 453, 543, 612, and 1119 cm^{-1} [22].

3.1.3. Surface analysis

Figs. 5 and 6 present the HRSEM images of the L24- and L48-coated copper substrates at different magnification scales. The images in both figures clearly exhibited that the LDHs were successfully grown on the copper substrate. HRSEM images of the LDH-coated copper at high magnifications showed that the LDHs were flower-like in shape. However, L24 was flower-like with short leaves, and L48 was flower-like with big leaves. This result indicated the effect of reaction time on surface morphology. A cross-sectional view of the LDH-coated copper is shown in inner view of Fig 7, which confirms the growth of LDH on the Copper substrate. Furthermore, the chemical compositions of the LDH coatings were analyzed by EDAX (Fig. 7). Both types of coatings were composed of copper with Mg, Zn, C, and O atoms. However, the weight percentages of Zn and Mg were

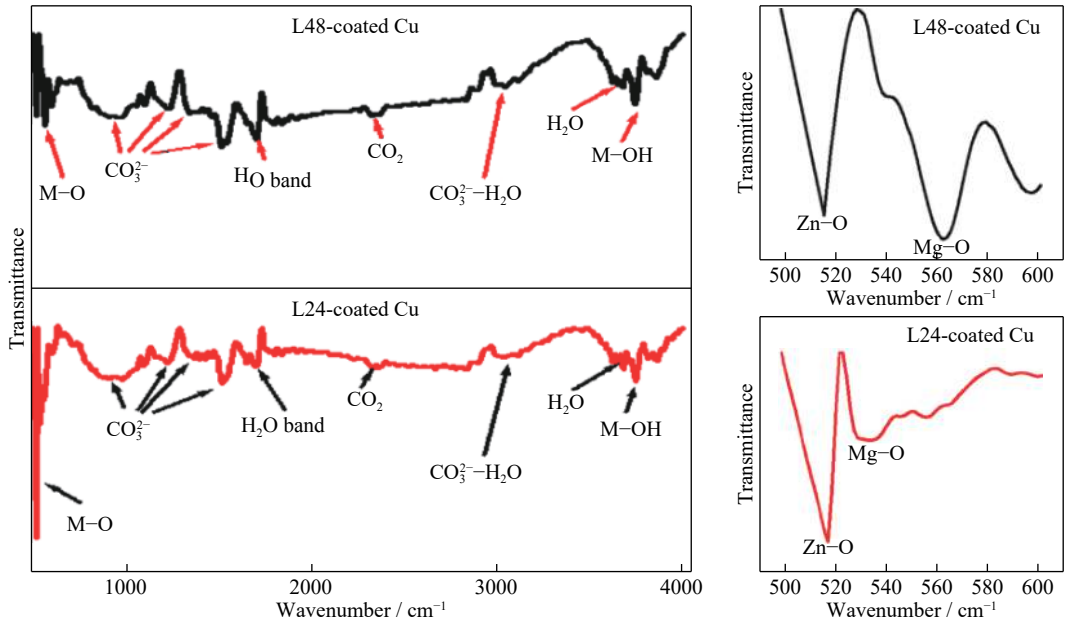

Fig. 3. FTIR spectra (left) and zoom in view of spectra (right) for L24 and L48 LDH coatings.

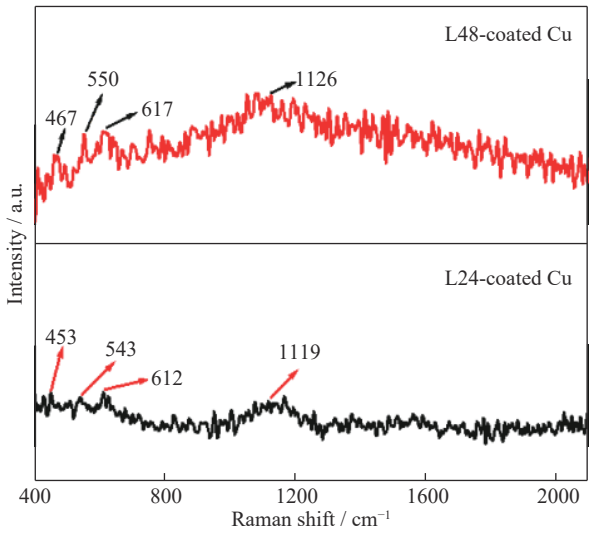

Fig. 4. Raman spectra of L24 and L48 LDH coatings.

higher in the L48 coatings than in the L24 coatings. This result confirmed that LDH growth was a function of time, which was obviously expected. The presence of C and O could indicate the presence of carbonates in the coatings.

Fig. 8 presents the 2-dimensional (2D) and 3-dimensional (3D) AFM images of copper and LDH (L24 and L48) coatings. Investigation of 2D images revealed that the LDH coatings were grown on the copper substrate. The height scale for L24 was approximately 300 nm, whereas that for L48 was 500 nm. This result clarified that the LDH coatings grew (size) more in 48 h than in 24 h. Three-dimensional AFM images (*x* and *y* axis in μm; and *z* axis in nm) of the copper and LDH coatings portrayed that the growth of the LDH molecules differed between 48 and 24 h. The average surface

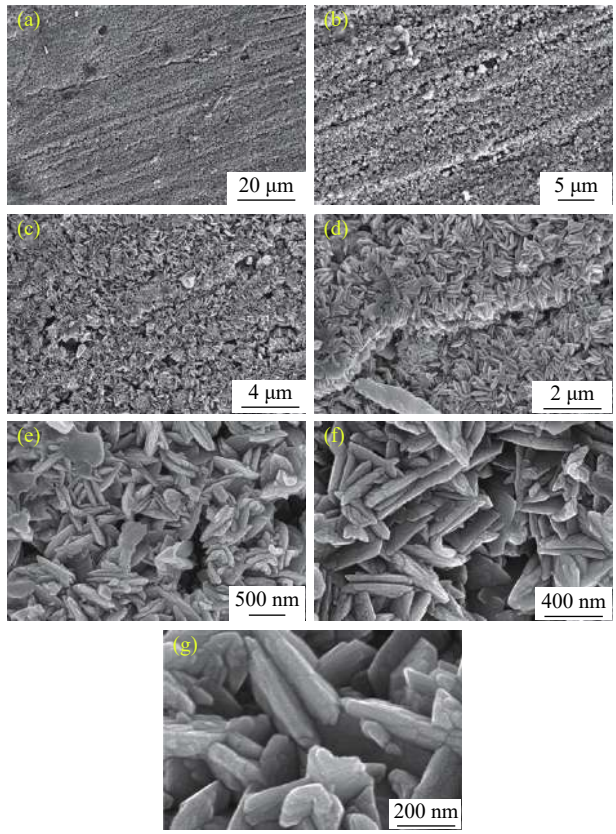

Fig. 5. HRSEM images of LDH coating (L24) at different magnifications.

roughness values for copper, L24, and L48 were 6, 84, and 93 nm, respectively. Thus, the results of surface analysis showed that different thicknesses of LDH coatings were grown on copper in 24 and 48 h.

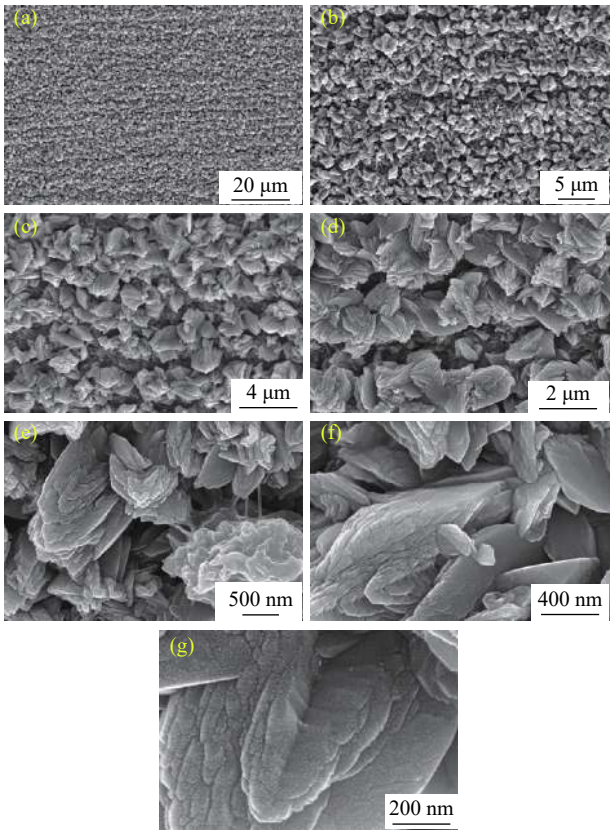

Fig. 6. HRSEM images of LDH coating (L48) at different magnifications.

3.2. Corrosion analysis

3.2.1. TPC test

Fig. 9 shows the TPCs for the copper and LDH-coated copper substrates in both test solutions. As shown in Fig. 9, the LDH-coated copper substrates provided lower corrosion current in the test solutions than pristine copper, which indicated that the LDH coatings were protective in nature [23–24]. Close investigation of Fig. 9 also disclosed that the nature of the cathodic polarization curves did not change much for the LDH coatings, but the anodic polarization curves changed drastically for the LDH coatings. This result indicated that the LDH coatings were more effective on anodic corrosion reactions (dissolution of copper) than on cathodic corrosion reactions [25]. Further inspection of TPC disclosed that the LDH coatings exhibited lower corrosion current in NaCl than in NaOH, which suggested that the LDH coatings were more protective in Cl^- environment than in OH^- environment.

For details, the polarization curves were extrapolated and various parameters related to corrosion were obtained. The main dynamic parameters were equilibrium corrosion potential, E_{corr}; corrosion current density, i_{corr}; slope of anodic TPC, b_a; and slope of cathodic TPC, b_c. As shown in Table 1, E_{corr} moved toward the positive direction in NaCl and in mixed direction in NaOH. This result demonstrated that the LDH coatings were more effective on anodic reactions in NaCl. However, the change in E_{corr} was within 85 mV in any case, which indicated that the LDH coatings acted as an effective barrier to anodic and cathodic corrosion reactions [26–27]. This result suggested that the LDH coatings mitigated the reduction of chemical species and the oxidation of copper. Further analysis of Table 1 revealed that the corrosion current densities for the LDH-coated copper substrates were much lower than those for pure copper. The corrosion current densities (i_{corr}) of the L24 and L48 coatings in NaCl were reduced up to 12 and 25 times, respectively, but only up to 6 and 13 times in NaOH, respectively. This result indicated that the LDH coatings were more effective reducing copper corrosion (weight ratio) in NaCl solution (96%) than in NaOH solution (93%). Moreover, the L48 coatings performed better than the L24 coatings in both test solutions. After analysis of the slope values of the polarization curves, both b_a and b_c changed values for the LDH-coated copper. However, changes in b_a were higher than those in b_c, indicating that the LDH coatings were more effective for lowering anodic corrosion reactions [28].

3.2.2. AIM analysis

Fig. 10 shows the Nyquist and Bode phase angle plots for the copper and LDH-coated copper substrates in both test solutions. The Nyquist plots were composed of either single semi-circle or double semi-circle in both test solutions. This

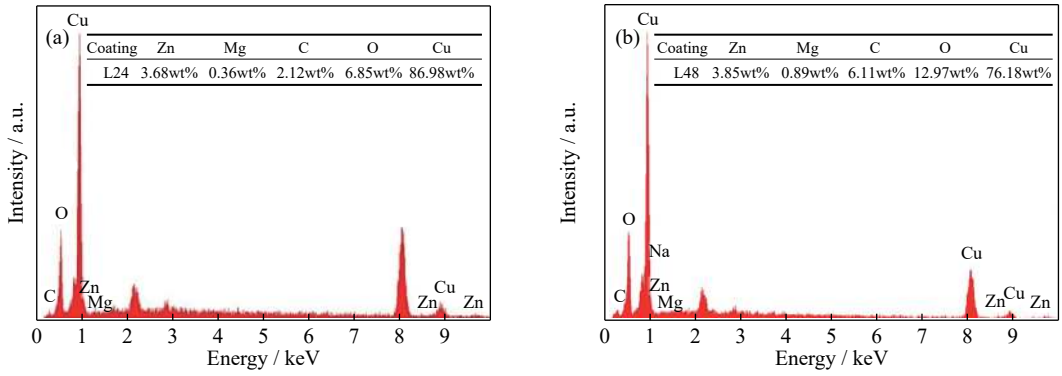

Fig. 7. EDAX spectra of (a) L24 and (b) L48 LDH coatings.

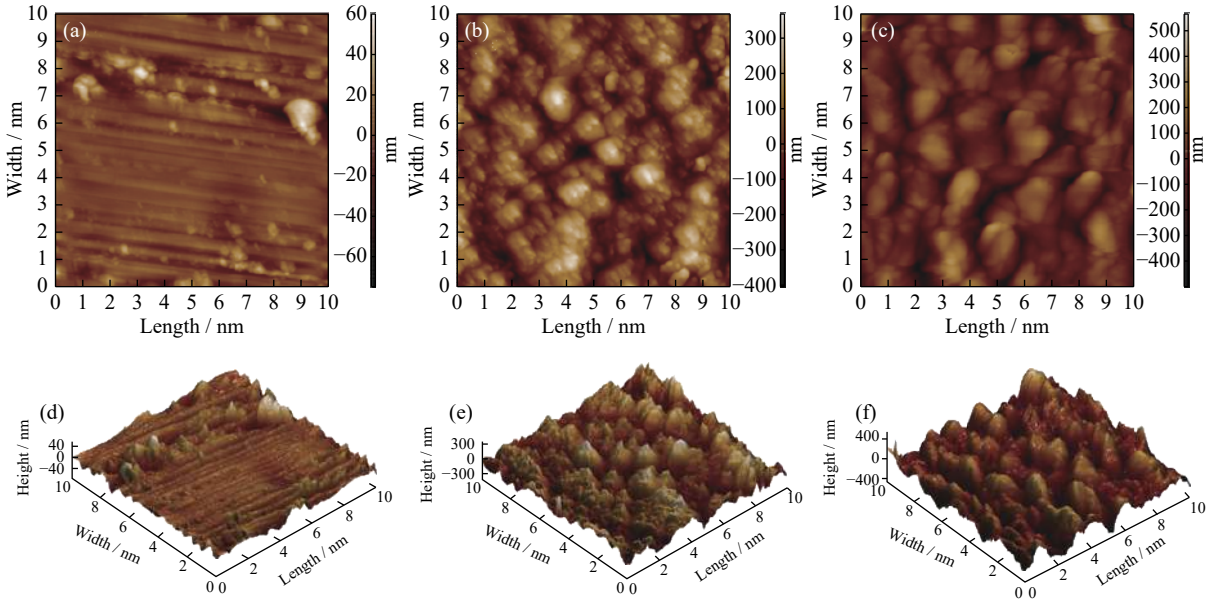

Fig. 8. 2D and 3D AFM images of (a, d) polished copper substrate, (b, e) L24, and (c, f) L48 LDH coatings.

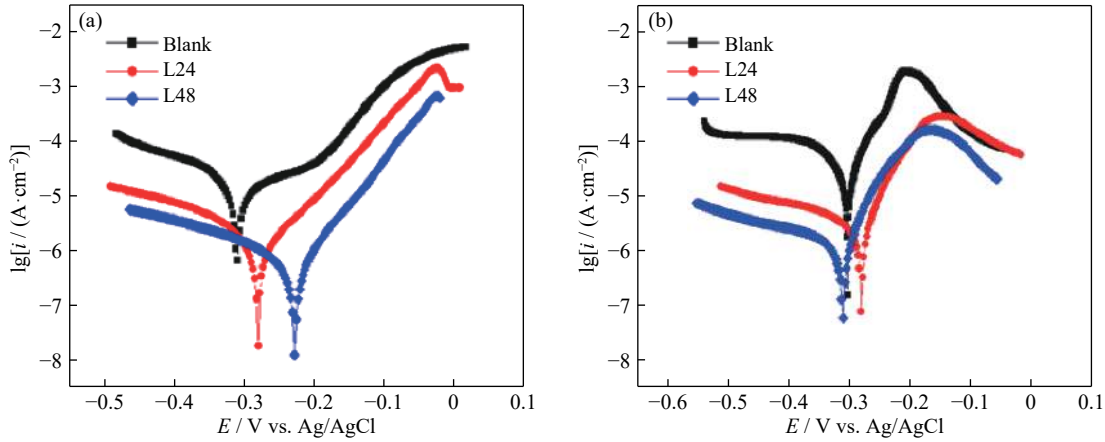

Fig. 9. Tafel polarization curves for copper, L24, and L48 LDH coatings in (a) 0.1 M NaCl and (b) 0.1 M NaOH at 24±2°C.

Table 1. Values of different parameters obtained by extrapolation of Tafel polarization curves for copper and LDH coatings in 0.1 M NaCl and 0.1 M NaOH at 24±2°C

Test solution	Exposure condition	i_{corr} / (A·cm^{-2})	$-E_{corr}$ / mV vs. Ag/AgCl	b_a / (mV·dec^{-1})	$-b_c$ / (mV·dec^{-1})	η_{PI} / %
NaCl	Blank	1.6×10^{-5}	0.28	190	232	—
	L24	1.3×10^{-6}	0.26	73	182	92
	L48	6.3×10^{-7}	0.21	57	220	96
NaOH	Blank	1.7×10^{-5}	0.30	74	42	—
	L24	2.5×10^{-6}	0.27	37	317	85
	L48	1.2×10^{-6}	0.29	42	304	93

result implied that the compositional structure of the coatings was not the same everywhere on the surface. Thus, a complete semi-circle was not observed in the *X*–*Y* plane. The Nyquist plots for the LDH coatings were much larger than those for pure copper, which indicated that the coatings effectively prevented copper from corrosion [29–30]. However, the Nyquist plots for the LDH coatings were larger in NaCl than in NaOH, indicating that the coatings were more efficient in NaCl solution than in NaOH solution. The Nyquist plots for the L24 coatings were smaller than those for the L48 coatings in both test solutions. Furthermore, Bode phase angle plots for the copper and L24-coated copper substrates exhibited that copper corrosion was clearly a two-step process. However, it was not clear for the Bode phase angle

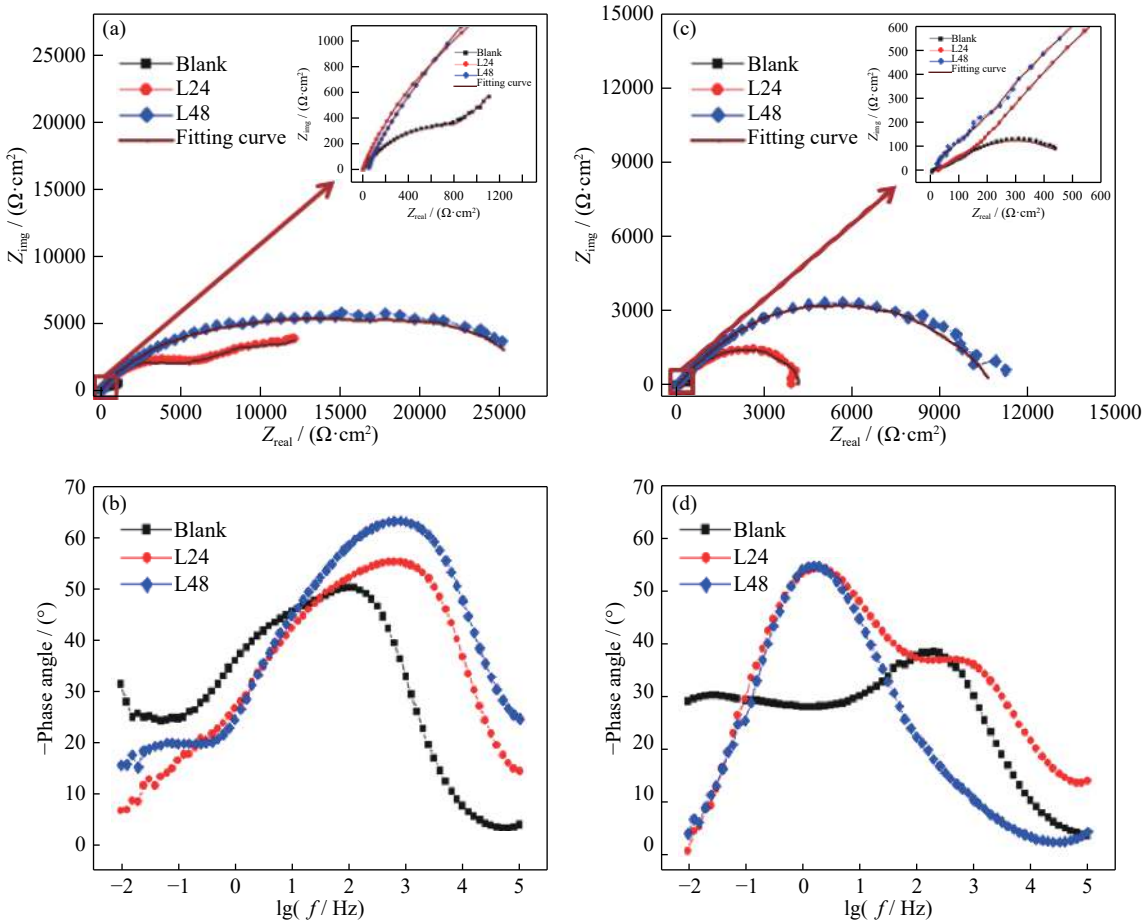

Fig. 10. Impedance curves of Copper, L24, and L48 LDH coatings in form of Nyquist and Bode plots (a, b) in 0.1 M NaCl and (c, d) in 0.1 M NaOH at 24±2°C. Inset (a, c): Zoom view of Nyquist plots.

plots of the L48-coated copper. Furthermore, the Bode phase angle at high frequency represents a general corrosion behavior of an electrochemical system [31]. A more negative value of the phase angle represents a more capacitive behavior of the system. Due to increased charge transfer resistance, the current has a natural tendency to pass through the capacitor in the circuit, casing the high capacitive behavior of the system. The high capacitive behavior of any system is preferable because it corresponds to high-quality (compactness and smoothness) film on the base substrate and thus high corrosion inhibition. In the present study, the Bode phase angles were higher for the LDH-coated copper than for pure copper, indicating that the LDH-coated copper was less corroded in both test solutions [32].

Nyquist plots were fitted using equivalent electrical circuit models (EECM), as shown in Fig. 11, to understand copper's corrosion in NaCl and NaOH solutions. Fig. 11(a) shows the corrosion behavior of copper in blank 0.1 M NaCl, whereas Fig. 11(b) displays the corrosion behavior of copper in 0.1 M NaOH. The corrosion behavior of the LDH coatings in both test media is shown in Fig. 11(c). The elements of EECM could be defined as follows: resistance of test solution, R_s; constant phase element capacitance of oxide film, Q_o; resistance of oxide film, R_o; constant phase element capacitance of LDH coating, Q_f; resistance of LDH film, R_f; constant phase element capacitance of double layer due to charge transfer, Q_{ct}; resistance of double layer against charge transfer, R_{ct}; and Warburg impedance, W_1. In EECM, W_1 is used to show transport of ions through oxide layers [33–34]; j is equal to $\sqrt{-1}$, ω is circular natural frequency, and α is a deviation factor. The EECM suggested the presence of two layers on copper: oxide layers/LDH coatings on copper and double layers formed between the electrolyte and copper. The total impedance (Z) in case of Figs. 10(a)–10(c) can be defined with the Eqs. (3)–(5):

$$Z = R_s + \cfrac{1}{(j\omega)^{\alpha} Q_o + \cfrac{1}{R_o + \cfrac{1}{(j\omega)^{\alpha} Q_{ct} + \cfrac{1}{R_{ct} + \cfrac{(1-j)W_1}{\sqrt{\omega}}}}}}, \quad \text{pure NaCl} \tag{3}$$

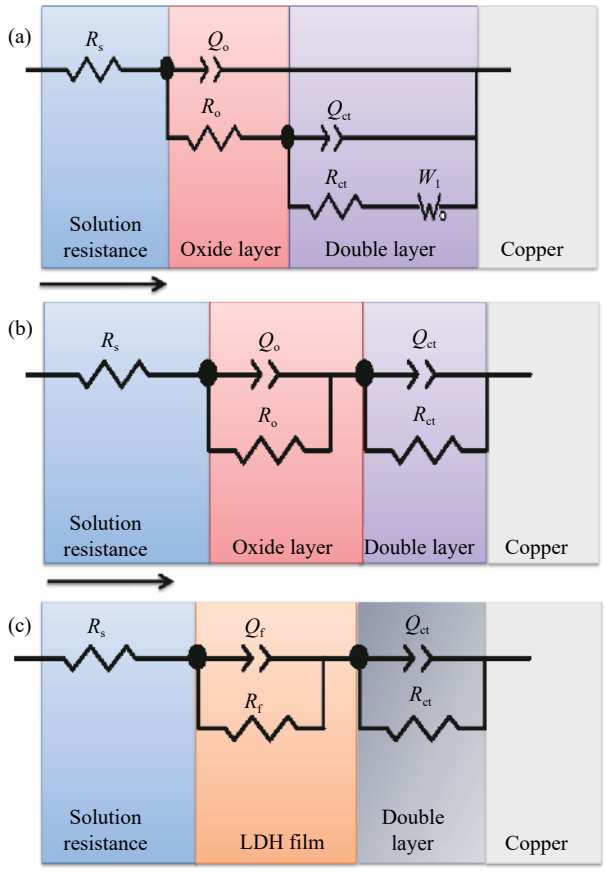

Fig. 11. EECM for corrosion behavior of copper in (a) 0.1 M NaCl and (b) 0.1 M NaOH, and (c) EECM for corrosion behavior of LDH coating-coated copper (L24 and L48) in both test solutions.

$$Z = R_s + \frac{1}{(j\omega)^{\alpha} Q_o + \frac{1}{R_o}} + \frac{1}{(j\omega)^{\alpha} Q_{ct} + \frac{1}{R_{ct}}}, \text{ pure NaOH} \quad (4)$$

$$Z = R_s + \frac{1}{(j\omega)^{\alpha} Q_f + \frac{1}{R_f}} + \frac{1}{(j\omega)^{\alpha} Q_{ct} + \frac{1}{R_{ct}}}, \text{ LDH coatings} \quad (5)$$

Table 2 presents the data obtained from the fitting of Nyquist curves by EECM. As per the EECM, pure copper strips in chloride and hydroxide media have one oxide layer and one double layer. Both layers corresponded to the corrosion of pure copper. The LDH-coated copper strips have one LDH film and one double layer. The LDH film over copper corresponded to corrosion protection, and the double layer is related to copper corrosion. The Q_f values of L24 and L48 were much lower than the Q_0 of pure copper in both solutions, which indicated that the LDH film was more compact than the oxide layer. In addition, the R_f values of L24 and L48 were much higher than the R_o of pure copper in both solutions, which suggested that the LDH film was more resistant to corrosion than the oxide layer. Increase in resistance and decrease in capacitance indicated that the LDH film provided better corrosion protection to copper than its oxide [35]. Thus, the L24- and L48-coated copper provided sufficient protection to copper substrate. The Q_{ct} values were higher in the blank copper than in the coated copper, which suggested that more damage occurred in the blank solutions. The R_{ct} values for the coated substrates were high compared with those for the uncoated copper, which indicated that coating effectively inhibited the corrosion of copper in the test solutions. The χ^2 (goodness of fitting) values and Z_{error} (fitting error in total impedance) were low, which indicated that the discussion based on the selected EECM was reliable. However, a slight variation in electrolyte resistance was observed, which could correspond to the variation in the thickness of the working electrodes. It was pure copper in one case and LDH-coated strips in the other case. Furthermore, L24 and L48 have different thicknesses. Overall, the impedance measurements suggested that the LDH coatings effectively protected copper corrosion in the NaCl and NaOH solutions.

3.3. Protection mechanism

Generally coatings serve as a physical barrier against corrosion and stop corrosive molecules to reach metal substrates. Coatings also provide chemical inertness to underlying metal substrates. A coating could act as a physical and chemical barrier. However, the basic reason of protection in any case is the isolation of metals from the working environment. A schematic of copper corrosion in NaCl and NaOH and of protection by LDH coatings in the same media is shown in Fig. 12. As explained by this mechanism, the corrosion of copper resulted in the formation of oxide/chloride layers on the surface. The surface copper molecules reacted with

Table 2. Values of different EECM elements obtained by fitting impedance curves for copper and LDH coatings in 0.1 M NaCl and 0.1 M NaOH at 24±2°C

Test solution	Exposure condition	R_s / ($\Omega \cdot cm^2$)	(Q_f/Q_o) / ($S.s^{\alpha_1}$)	α_1	(R_f/R_o) / ($\Omega \cdot cm^2$)	Q_{ct} / ($S.s^{\alpha_2}$)	α_2	R_{ct} / ($\Omega \cdot cm^2$)	W_1 / ($\times 10^{-3}$ $\Omega \cdot s^{-1/2}$)	η_{Rct} / %	χ^2 / 10^{-3}	Z_{error} / %
NaCl	Blank	9	111	0.77	155	376	0.67	666	43	—	4.3	6.4
	L24	8	17	0.72	5403	287	0.67	11170	—	95	3.0	5.4
	L48	46	11	0.68	8025	52	0.65	18780	—	97	2.5	5.0
NaOH	Blank	4	300	0.77	27	3261	0.53	577	—	—	1.2	3.5
	L24	22	197	0.53	188	218	0.73	4262	—	82	1.3	3.6
	L48	46	76	0.54	504	59	0.72	14790	—	94	1.7	4.1

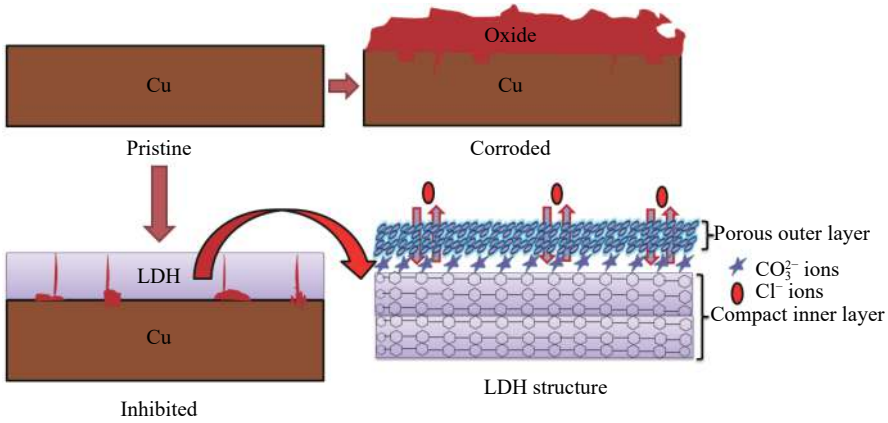

Fig. 12. Schematic for corrosion protection of copper in chloride media by LDH coatings.

Cl^-/OH^- ions and formed copper chlorides/hydroxides. These layers do not provide sufficient protection; hence, corrosive solutions can still reach the copper substrate through porous layers (micro pores). Thus, the corrosion of copper occurs continuously. The LDH coatings presented in this study can provide sufficient protection to copper substrate.

Some papers [9–10,36] discussed the protection mechanism of LDH in detail. All LDHs have unified formula and fixed chemical structure. Hence, they provide protection to metals by similar means. The protection mechanism of LDH in our case could be linked to those works for explanation. LDH coatings have two layers of metal cations, and anions are intercalated between metal cation layers in the gallery of LDH. On exposure, LDH starts exchange of its anions (in present case, CO_3^{2-} ions) with corrosive anions (Cl^-/OH^-) first [16]. Due to this exchange, some corrosive ions are captured in LDH and thus reduce the aggressiveness of corrosive solutions [13–14]. Then, metal cations (in present case, Zn^{2+} and Mg^{2+} ions) released from the scaffold of LDH interact with anions to form protective oxides for protection of base substrate through self-healing effect [13–14]. Thus, the LDH used in this work can provide protection through chloride/hydroxyl anion ion entrapment and metal cation release [9–10,36]. However, results of corrosion tests showed that the LDH coatings were more effective in NaCl than in NaOH. Possible reasons could be the easier exchange of Cl^- ions with the CO_3^{2-} ions of LDH coatings than with the OH^- ions and the easier release of metal cations in NaCl solution than in NaOH solution. In addition, the OH^- ions introduced more cracks (pores) in the LDH coatings, which helped the OH^- ions to reach the copper substrate. This assumption could be supported by the higher Q_f/Q_o values obtained for the LDH coatings in NaOH than in NaCl.

4. Conclusion

This work deals with the LDH formation on the copper substrate for its corrosion protection in NaCl and NaOH media. Two types of Zn–Mg-based LDHs were developed on copper substrate: L24 and L48. The major difference between these two LDHs was thickness of coating (L48>L24). These coatings were characterized through various techniques, which confirmed the formation of LDH coating on the top of the copper substrate. The corrosion performances of the LDH coatings were assessed in 0.1 M NaCl and NaOH. Results showed that the LDH coatings were effective in the corrosion protection of copper. However, the protection ability of the LDH coatings was higher in NaCl than in NaOH. The results of corrosion testing showed that the LDH coatings provided good protection ability in acidic and basic media (>90%). Thus, the protection ability of LDH was not considerably affected by the nature of corrosive solutions. Hence, LDH coatings could be recommended for the protection of cooper in chloride and hydroxide media.

Acknowledgements

Dr. Gopal Ji wants to acknowledge the support of lab mates of IIT BHU Varanasi and Colleagues of Centre for Advanced studies (APJAKTU Lucknow).

References

[1] Y. Jafari, S.M. Ghoreishi, and M. Shabani-Nooshabadi, Polyaniline/graphene nanocomposite coatings on copper: Electropolymerization, characterization, and evaluation of corrosion protection performance, *Synth. Met.*, 217(2016), p. 220.

[2] D.Q. Zhang, Q.R. Cai, X.M. He, L.X. Gao, and G.D. Zhou, Inhibition effect of some amino acids on copper corrosion in HCl solution, *Mater. Chem. Phys.*, 112(2008), No. 2, p. 353.

[3] E.S.M. Sherif, Corrosion mitigation of copper in acidic chloride pickling solutions by 2-amino-5-ethyl-1,3,4-thiadiazole, *J. Mater. Eng. Perform.*, 19(2010), No. 6, p. 873.

[4] D.Q. Zhang, B. Xie, L.X. Gao, Q.R. Cai, H.G. Joo, and K.Y. Lee, Intramolecular synergistic effect of glutamic acid, cysteine and glycine against copper corrosion in hydrochloric acid solution, *Thin Solid Films*, 520(2011), No. 1, p. 356.

[5] A.Y. El-Etre, Natural honey as corrosion inhibitor for metals and alloys. I. Copper in neutral aqueous solution, *Corros. Sci.*,

40(1998), No. 11, p. 1845.
[6] N.A. Wazzan, DFT calculations of thiosemicarbazide, arylisothiocynates, and 1-aryl-2,5-dithiohydrazodicarbonamides as corrosion inhibitors of copper in an aqueous chloride solution, *J. Ind. Eng. Chem.*, 26(2015), p. 291.
[7] N. Karthik, Y.R. Lee, and M.G. Sethuraman, Hybrid sol–gel/thiourea binary coating for the mitigation of copper corrosion in neutral medium, *Prog. Org. Coat.*, 102(2017), p. 259.
[8] R. Farahati, A. Ghaffarinejad, S.M. Mousavi-Khoshdel, J. Rezania, H. Behzadi, and A. Shockravi, Synthesis and potential applications of some thiazoles as corrosion inhibitor of copper in 1 M HCl: Experimental and theoretical studies, *Prog. Org. Coat.*, 132(2019), p. 417.
[9] E. Alibakhshi, E. Ghasemi, M. Mahdavian, B. Ramezanzadeh, and S. Farashi, Active corrosion protection of Mg–Al–PO_4^{3-} LDH nanoparticle in silane primer coated with epoxy on mild steel, *J. Taiwan Inst. Chem. Eng.*, 75(2017), p. 248.
[10] E. Alibakhshi, E. Ghasemi, M. Mahdavian, and B. Ramezanzadeh, A comparative study on corrosion inhibitive effect of nitrate and phosphate intercalated Zn–Al-layered double hydroxides (LDHs) nanocontainers incorporated into a hybrid silane layer and their effect on cathodic delamination of epoxy topcoat, *Corros. Sci.*, 115(2017), p. 159.
[11] E. Alibakhshi, E. Ghasemi, M. Mahdavian, and B. Ramezanzadeh, Fabrication and characterization of layered double hydroxide/silane nanocomposite coatings for protection of mild steel, *J. Taiwan Inst. Chem. Eng.*, 80(2017), p. 924.
[12] G. Mishra, B. Dash, S. Pandey, and D. Sethi, Ternary layered double hydroxides (LDH) based on Cu-substituted Zn–Al for the design of efficient antibacterial ceramics, *Appl. Clay Sci.*, 165(2018), p. 214.
[13] R.C. Zeng, X.T. Li, Z.G. Liu, F. Zhang, S.Q. Li, and H.Z. Cui, Corrosion resistance of Zn–Al layered double hydroxide/poly(lactic acid) composite coating on magnesium alloy AZ_{31}, *Front. Mater. Sci.*, 9(2015), No. 4, p. 355.
[14] F. Zhang, Z.G. Liu, R.C. Zeng, S.Q. Li, H.Z. Cui, L. Song, and E.H. Han, Corrosion resistance of Mg–Al-LDH coating on magnesium alloy AZ31, *Surf. Coat. Technol.*, 258(2014), p. 1152.
[15] J.K. Lin, K.L. Jeng, and J.Y. Uan, Crystallization of a chemical conversion layer that forms on AZ91D magnesium alloy in carbonic acid, *Corros. Sci.*, 53(2011), No. 11, p. 3832.
[16] J.K. Lin, C.L. Hsia, and J.Y. Uan, Characterization of Mg,Al-hydrotalcite conversion film on Mg alloy and Cl^- and CO_3^{2-} anion-exchangeability of the film in a corrosive environment, *Scr. Mater.*, 56(2007), No. 11, p. 927.
[17] G. Ji, S.K. Shukla, P. Dwivedi, S. Sundaram, and R. Prakash, Inhibitive effect of argemone mexicana plant extract on acid corrosion of mild steel, *Ind. Eng. Chem. Res.*, 50(2011), No. 21, p. 11954.
[18] G. Ji, P. Dwivedi, S. Sundaram, and R. Prakash, Inhibitive effect of chlorophytum borivilianum root extract on mild steel corrosion in HCl and H_2SO_4 solutions, *Ind. Eng. Chem. Res.*, 52(2013), No. 31, p. 10673.
[19] M. Tiwari, V.K. Gupta, R.A. Singh, G. Ji, and R. Prakash, Donor–π–acceptor-type configured, dimethylamino-based organic push–pull chromophores for effective reduction of mild steel corrosion loss in 1 M HCl, *ACS Omega*, 3(2018), No. 4, p. 4081.
[20] T. Ishizaki, S. Chiba, K. Watanabe, and H. Suzuki, Corrosion resistance of Mg–Al layered double hydroxide container-containing magnesium hydroxide films formed directly on magnesium alloy by chemical-free steam coating, *J. Mater. Chem. A*, 1(2013), No. 31, p. 8968.
[21] L.D. Wang, K.Y. Zhang, W. Sun, T.T. Wu, H.R. He, and G.C. Liu, Hydrothermal synthesis of corrosion resistant hydrotalcite conversion coating on AZ91D alloy, *Mater. Lett.*, 106(2013), p. 111.
[22] J.T. Kloprogge, L. Hickey, and R.L. Frost, FT-Raman and FT-IR spectroscopic study of synthetic Mg/Zn/Al-hydrotalcites, *J. Raman Spectrosc.*, 35(2004), No. 11, p. 967.
[23] P. Tiwari, M. Srivastava, R. Mishra, G. Ji, and R. Prakash, Economic use of waste Musa paradisica peels for effective control of mild steel loss in aggressive acid solutions, *J. Environ. Chem. Eng.*, 6(2018), No. 4, p. 4773.
[24] M. Srivastava, P. Tiwari, S.K. Srivastava, A. Kumar, G. Ji, and R. Prakash, Low cost aqueous extract of Pisum sativum peels for inhibition of mild steel corrosion, *J. Mol. Liq.*, 254(2018), p. 357.
[25] G. Ji, S. Anjum, S. Sundaram, and R. Prakash, Musa paradisica peel extract as green corrosion inhibitor for mild steel in HCl solution, *Corros. Sci.*, 90(2015), p. 107.
[26] E.S. Ferreira, C. Giacomelli, F.C. Giacomelli, and A. Spinelli, Evaluation of the inhibitor effect of $_L$-ascorbic acid on the corrosion of mild steel, *Mater. Chem. Phys.*, 83(2004), No. 1, p. 129.
[27] W.H. Li, Q. He, S.T. Zhang, C.L. Pei, and B.R. Hou, Some new triazole derivatives as inhibitors for mild steel corrosion in acidic medium, *J. Appl. Electrochem.*, 38(2008), No. 3, p. 289.
[28] G. Ji, P. Dwivedi, S. Sundaram, and R. Prakash, Aqueous extract of *Argemone mexicana* roots for effective protection of mild steel in an HCl environment, *Res. Chem. Intermed.*, 42(2016), No. 2, p. 439.
[29] T.F. Xiang, S.L. Zheng, M. Zhang, H.R. Sadig, and C. Li, Bioinspired slippery zinc phosphate coating for sustainable corrosion protection, *ACS Sustainable Chem. Eng.*, 6(2018), No. 8, p. 10960.
[30] H. Lgaz, R. Salghi, S. Jodeh, and B. Hammouti, Effect of clozapine on inhibition of mild steel corrosion in 1.0 M HCl medium, *J. Mol. Liq.*, 225(2017), p. 271.
[31] E. Alibakhshi, E. Ghasemi, M. Mahdavian, B. Ramezanzadeh, and M. Yasaei, The effect of interlayer spacing on the inhibitor release capability of layered double hydroxide based nanocontainers, *J. Cleaner Prod.*, 251(2020), art. No. 119676.
[32] M.M. Solomon, S.A. Umoren, and E.J. Abai, Poly(methacrylic acid)/silver nanoparticles composites: *In-situ* preparation, characterization and anticorrosion property for mild steel in H_2SO_4 solution, *J. Mol. Liq.*, 212(2015), p. 340.
[33] G. Ji, L.F. Macía, B. Allaert, A. Hubin, and H. Terryn, Odd random phase electrochemical impedance spectroscopy to study the corrosion behavior of hot dip Zn and Zn-alloy coated steel wires in sodium chloride solution, *J. Electrochem. Soc.*, 165(2018), No. 5, p. 246.
[34] M.A. Arenas, I. García, and J. de Damborenea, X-ray photoelectron spectroscopy study of the corrosion behaviour of galvanised steel implanted with rare earths, *Corros. Sci.*, 46(2004), No. 4, p. 1033.
[35] C. Deslouis, M. Duprat, and C. Tournillon, The kinetics of zinc dissolution in aerated sodium sulphate solutions. A measurement of the corrosion rate by impedance techniques, *Corros. Sci.*, 29(1989), No. 1, p. 13.
[36] J.X. Xu, Y.B. Song, Y.H. Zhao, L.H. Jiang, Y.J. Mei, and P. Chen, Chloride removal and corrosion inhibitions of nitrate, nitrite-intercalated Mg–Al layered double hydroxides on steel in saturated calcium hydroxide solution, *Appl. Clay Sci.*, 163(2018), p. 129.